Electrochemistry

DOI: 10.1002/anie.201302577

Electrochemically Mediated Seawater Desalination**

Kyle N. Knust, Dzmitry Hlushkou, Robbyn K. Anand, Ulrich Tallarek, and Richard M. Crooks**

With global demand rising faster than availability, fresh water is quickly becoming a limited resource. In fact, the United Nations estimates one third of the world's population is living in water-stressed regions, and by 2025 this number is expected to double.[1] Seawater desalination is an attractive solution to this problem because seawater accounts for more than 97% of the world's water supply.[2] Currently, the primary limitation preventing the widespread use of seawater desalination as a fresh water supply is the immense amount of energy required to drive the process.[3] Here, we describe a new, electrochemically mediated desalination (EMD) method for membraneless seawater desalination.

Our approach for desalination is illustrated in Figure 1a. A seawater feed is separated into brine and desalted water streams at the junction of a branched microchannel where a bipolar electrode (BPE)[4] is present. The anodic pole of the BPE generates an ion depletion zone,[5] and hence a local electric field gradient that redirects ions present in seawater to the brine channel. Importantly, this device operates with an energy efficiency of 25 $mWhL^{-1}$ ($25\pm5\%$ salt rejection, 50% recovery), which is near the theoretical minimum amount of energy required for this process (ca. 17 $mWhL^{-1}$).[6] In addition to this energy efficiency, the approach provides three other important benefits relative to currently available desalination methods. First, EMD does not require a membrane, thereby eliminating a major drawback of reverse osmosis (RO), the most widespread method for desalination.[7] Second, EMD requires only a simple 3.0 V power supply to operate and therefore, in the future, may be employed in resource-limited settings with a battery or low-power, renewable energy source. Third, the EMD platform may be prepared with little capital investment and could be implemented in a massively parallel format.[8]

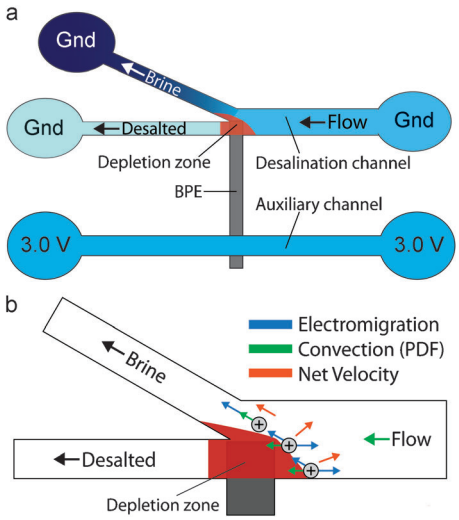

Figure 1. Schematic illustrations of a) the BPE desalination device and b) the region of interest near the BPE anode and ion depletion zone depicting the net velocity vectors of a cationic species under the combined forces of electromigration and convection. Gnd = ground.

Our groups have developed microfluidic technologies using BPEs for the enrichment,[9] separation,[10] depletion,[11] and controlled delivery[12] of charged analytes. In all cases, the approach relies on the formation of a locally generated electric field gradient and control over convection. The basic operating principles of BPEs[13] and how they are able to generate electric field gradients have been previously described.[14] Briefly, if a sufficiently high potential bias (E_{tot}) is applied across a microfluidic channel in which a BPE is present, faradaic reactions will occur at the BPE poles. In seawater, these faradaic reactions result in the formation of an ion depletion zone (region of high solution resistivity), thus producing a local electric field gradient and providing a means for controlling the movement of ions.[15]

Several other techniques, including dynamic field gradient focusing[16] and electric field gradient focusing,[17] also rely on a gradient in the electric field to control the transport of charged analytes. Most relevant to this work is a phenomenon called ion concentration polarization (ICP),[18] which generates an ion depletion zone when a potential bias applied across two fluidic channels causes a large proportion of ionic

[*] K. N. Knust, Dr. R. K. Anand, Prof. R. M. Crooks
Department of Chemistry and the Center for Nano- and Molecular Science and Technology, The University of Texas at Austin
105 E. 24th St., Stop A5300, Austin, TX 78712-0165 (USA)
E-mail: crooks@cm.utexas.edu
Dr. D. Hlushkou, Prof. U. Tallarek
Department of Chemistry, Philipps-Universität Marburg
Hans-Meerwein-Strasse, 35032 Marburg (Germany)
E-mail: tallarek@staff.uni-marburg.de

[**] We acknowledge the Chemical Sciences, Geosciences, and Biosciences Division, Office of Basic Energy Sciences, Office of Science, U.S. Department of Energy (contract no. DE-FG02-06ER15758) for supporting the basic research that led to the development of this technology. We acknowledge financial support from Okeanos Technologies, LLC, for supporting certain aspects of the technological implementation. The Robert A. Welch Foundation provides sustained support for our research (Grant F-0032). We thank Prof. Don Paul (UT-Austin) for helpful discussions about desalination and Tim Hooper (UT-Austin) for providing technical assistance with the conductivity measurements. R.K.A. receives support from NIH training grant (NIH T32 CA138312). We thank the Deutsche Forschungsgemeinschaft (grant TA 268/5-1, DFG, Bonn (Germany)) for support of the simulations described herein.

Supporting information for this article is available on the WWW under http://dx.doi.org/10.1002/anie.201302577.

current to be carried by either anions or cations through a permselective material or a nanochannel exhibiting overlap of the electrical double layer. In fact, Han and co-workers have recently shown that ICP can be adapted to seawater desalination with a reported energy efficiency of 3750 mW h L^{-1} (ca. 99% salt rejection, 50% recovery) for a small-scale system.[19] A number of other electrochemical approaches, including capacitive deionization,[20] a desalination battery,[21] and electrodialysis,[22] have also been implemented for seawater desalination, although these techniques are more commonly used to desalinate brackish water because their power consumption scales with the extent of salt removal.[23]

The EMD experiments reported here were carried out by using a poly(dimethylsiloxane) (PDMS)/quartz hybrid microfluidic device (22 μm-tall channels with a 100 μm-wide inlet and two 50 μm-wide outlets) outfitted with a pyrolyzed photoresist carbon (PPC)[24] BPE. Additional details regarding the device design, fabrication, and characterization can be found in the Supporting Information. Both channels were filled with seawater collected near Port Aransas, Texas, USA. To prevent obstruction of the microfluidic channel, sand and debris present in the seawater sample were removed through sedimentation before use. Importantly, no other pre-treatment was required. This is in contrast to membrane-based desalination where further pre-treatment, such as disinfection and the addition of anti-scaling chemicals, is required to prevent fouling and maintain the structural integrity of the membrane.[25]

The experimental arrangement is shown in Figure 1a. In the desalination channel, seawater is spiked with a fluorescent cationic tracer, tris(2,2′-bipyridyl) ruthenium(II) chloride ($[Ru(bpy)_3]^{2+}$), representative of ionic motion. A total pressure driven flow (PDF) of approximately 0.08 μL min^{-1} is initiated between the inlet and outlets by creating a solution height differential between them. Next, using Pt driving electrodes dipped into each of the five reservoirs, $E_{tot} = 3.0$ V is applied. This creates a sufficiently large potential difference between the BPE poles to drive chloride oxidation and water reduction at the BPE anode and cathode, Equations (1) and (2), respectively. Importantly, chloride oxidation results in the neutralization of Cl^- and hence an ion depletion zone and local electric field gradient near the BPE anode.

$$2\,Cl^- - 2\,e^- \leftrightarrow Cl_2 \quad (1)$$

$$2\,H_2O + 2\,e^- \leftrightarrow H_2 + 2\,OH^- \quad (2)$$

Although chloride oxidation is known to be the dominant anodic process occurring in seawater,[26] water oxidation also occurs by Equation (3). Electrogenerated H^+ arising from water oxidation may neutralize anions present in seawater, such as bicarbonate and borate, thus further contributing to ion depletion and the electric field gradient.

$$2\,H_2O - 4\,e^- \leftrightarrow O_2 + 4\,H^+ \quad (3)$$

The electrophoretic velocity (u_{ep}) of an ion is governed by Equation (4), where μ_{ep} is its electrophoretic mobility and V_l is the local electric field strength.

$$u_{ep} = \mu_{ep} V_l \quad (4)$$

In all regions of the desalination channel depicted in Figure 1b, except near the ion depletion zone, ionic transport is dominated by PDF, which results in a net movement toward the outlets. However, as ions approach the local electric field gradient, they experience an increasing u_{ep}. At some point on this gradient, u_{ep} will exceed the convective velocity, and therefore cations will be directed toward the grounded reservoir in the brine stream. To maintain electroneutrality within the microchannel, anions are also redirected into the brine stream.

Figure 2 provides fluorescence micrographs confirming the electrochemically driven redirection of ions. In Figure 2a, the $[Ru(bpy)_3]^{2+}$ tracer, which represents the ions in seawater,

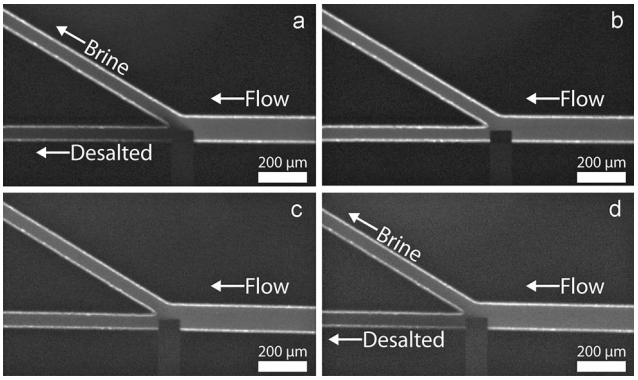

Figure 2. Fluorescence micrographs showing the location of the $[Ru(bpy)_3]^{2+}$ tracer, which is representative of the ions present in seawater. a) The tracer in seawater is redirected into the brine stream with $E_{tot} = 3.0$ V. b) Same as (a) except $E_{tot} = 0.0$ V. In this case, the tracer flows into both outlets. c) In 50 mS cm^{-1} Na_2SO_4, the tracer flows into both outlets with $E_{tot} = 3.0$ V. d) In 50 mS cm^{-1} NaCl, the tracer is redirected into the brine stream with $E_{tot} = 3.0$ V. In all cases, the total PDF was approximately 0.08 μL min^{-1}.

is selectively directed into the brine stream. Conversely, water flowing into the lower channel is depleted of tracer. During this desalination process, in situ conductivity measurements were performed using a procedure described in the Supporting Information. The average conductivity in the desalted stream from five individual trials was (37.5 ± 2.5) mS cm^{-1}, indicating a 25 ± 5% salt rejection from the feed seawater (50 mS cm^{-1}). The power source was then turned off (Figure 2b, $E_{tot} = 0.0$ V), whereupon the fluorescent tracer flowed into the desalted stream and the conductivity returned to 50 mS cm^{-1}. Although the salt rejection is lower than mature desalination technologies, the EMD process is far from optimized.

The experiment represented in Figure 2c was carried out exactly like that described for Figure 2a, but using 50 mS cm^{-1} Na_2SO_4 instead of seawater. The purpose of this experiment is to demonstrate that the formation of a local electric field gradient is essential for driving desalination. The Na_2SO_4 eliminates the possibility of an ion depletion zone forming due to Equation (1) or by the neutralization of weak bases present in seawater with electrogenerated H^+. In this case,

there is no selective redirection of $[Ru(bpy)_3]^{2+}$, thus emphasizing the importance of Cl^- for desalting. The slight decrease in fluorescence intensity in the desalted stream occurs as a result of O_2, generated by water oxidation, quenching the $[Ru(bpy)_3]^{2+}$ fluorescence.[27] Importantly, electric field measurements presented in the Supporting Information demonstrate that no local electric field gradient is observed in the presence of Na_2SO_4. Experiments were also carried out exactly like that described for Figure 2a, except with 50 mS cm^{-1} NaCl. In this case (Figure 2d), $[Ru(bpy)_3]^{2+}$ is redirected into the brine stream, clearly implicating Cl^- as a critical factor in the desalination process. Electric field measurements (Supporting Information) confirm the formation of a local electric field gradient in the presence of NaCl. The key point is that the formation of a local electric field gradient is necessary to induce EMD.

Numerical simulations were used to confirm our proposed mechanism for desalination. The simulations mirror the experiment corresponding to Figure 2d: desalination of a 50 mS cm^{-1} NaCl solution with the assumption of Cl^- oxidation at the BPE anode. Details regarding the theoretical background and numerical methods can be found in the Supporting Information. Figure 3a shows the simulated distribution of salinity in the region of interest close to the BPE anode, normalized by its value in the desalination channel inlet. The developed electric field gradient (Figure 3b,c) redirects ions toward the brine stream, resulting in a 20% reduction of salinity in the desalted stream. This result is in excellent agreement with the experimental findings (25 ± 5% salt rejection).

Figure 4 shows a representative plot of total current through the device versus time. The steady-state operating current was 20 nA (device-to-device variation was 10–80 nA) with $E_{tot} = 3.0$ V driving the desalination process, hence yielding a power consumption of 60 nW. The average flow rate of desalted water was approximately 0.04 μL min^{-1}, resulting in an energy efficiency of just 25 mW h L^{-1} for 25 ± 5% salt rejection at a 50% recovery. Thus, this device compares competitively with efficient, state-of-the-art seawater desalination technologies, such as RO, which typically operates at approximately 2000 mW h L^{-1} (ca. 99% salt rejection, 50% recovery) for a process that requires a theoretical minimum energy of approximately 1000 mW h L^{-1}.[28] Note that these RO efficiencies do not include the energy associated with seawater intake, pre-treatment required to maintain membrane performance, or post-treatment. Importantly, RO efficiency improves as the scale of the process is increased to incorporate energy recovery systems,[2a] and therefore the energy required to run small-scale RO desalination is higher than 2000 mW h L^{-1}. This suggests that EMD, powered by a 3.0 V battery pack (Supporting Information), could be competitive for small-scale applications and have utility in resource-limited settings.

The fundamental operating principles of EMD are different than those of membrane and thermal desalination technologies. For example, membrane-based desalination requires an applied pressure greater than the high osmotic pressure of seawater (ca. 30 atm) to desalt. With regard to thermal desalination, sufficient energy must be provided to

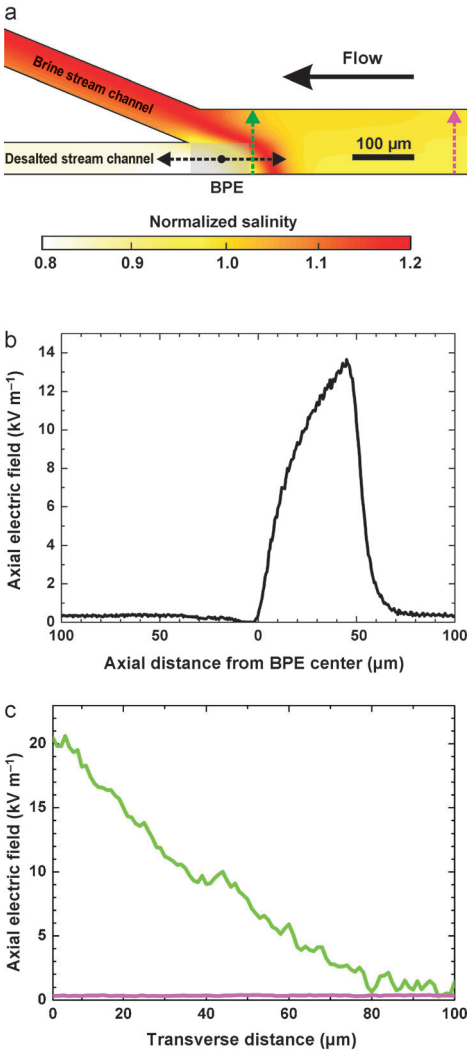

Figure 3. a) Local salinity distribution simulated for a 50 mS cm^{-1} NaCl solution with $E_{tot} = 3.0$ V and a total PDF rate of 0.08 μL min^{-1} from inlet to outlets; the current through the BPE is 50 nA. b) Simulated profile of the axial electric field strength along the centerline of the desalted stream (as indicated by the black arrows in (a)). c) Simulated profiles of the axial electric field strength along the transverse direction of the desalination channel (as indicated by the green and purple arrows in the corresponding color in (a)).

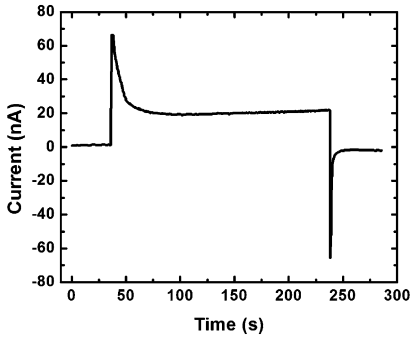

Figure 4. A plot of total current versus time during a seawater desalination experiment showing the steady-state operating current of 20 nA required to drive desalination. Both microchannels were filled with seawater. $E_{tot} = 3.0$ V was applied and the total PDF was approximately 0.08 μL min^{-1}.

vaporize water. In both cases, there are clearly defined minimum energy requirements. EMD requires only enough energy to oxidize a sufficient percentage of the total Cl^- ions present in seawater to generate the local electric field gradient. In the present configuration, this amounts to approximately 0.01% (Supporting Information). EMD does require PDF, but the power required for this gravity driven flow is negligible (112 pW, Supporting Information).

In summary, we have demonstrated a membraneless and energy efficient technique for seawater desalination. EMD relies on the oxidation of Cl^-, which generates an ion depletion zone and local electric field gradient to redirect sea salts into a brine stream. This result is important for a number of reasons. First, the technique is membraneless, and therefore does not suffer from membrane fouling or damage and does not require extensive pre-treatment prior to desalination. Second, EMD achieves energy efficiencies of $25\ mW\,h\,L^{-1}$ for $25\pm5\%$ salt rejection at a 50% recovery of desalted water (theoretical minimum energy efficiency is ca. $17\ mW\,h\,L^{-1}$). Lastly, the simple design, operation, and equipment required to perform EMD greatly reduces the capital costs associated with desalination. In the future, it may be possible to use arrays of channels and BPEs to increase the production of desalted water. Moreover, we believe there is considerable room for optimization of the channel and electrode designs.

Received: March 28, 2013
Published online: June 19, 2013

Keywords: desalination · electrochemistry · electrophoresis · microfluidics · water

[1] United Nations, World Water Development Report 2. **2006**.
[2] a) M. A. Shannon, P. W. Bohn, M. Elimelech, J. G. Georgiadis, B. J. Marinas, A. M. Mayes, *Nature* **2008**, *452*, 301 – 310; b) R. F. Service, *Science* **2006**, *313*, 1088 – 1090.
[3] M. Hightower, S. A. Pierce, *Nature* **2008**, *452*, 285 – 286.
[4] S. E. Fosdick, K. N. Knust, K. Scida, R. M. Crooks, *Angew. Chem.* **2013**, DOI: 10.1002/ange.201300947; *Angew. Chem. Int. Ed.* **2013**, DOI: 10.1002/anie.201300947.
[5] R. K. Anand, E. Sheridan, K. N. Knust, R. M. Crooks, *Anal. Chem.* **2011**, *83*, 2351 – 2358.
[6] a) Y. A. Cengel, Y. Cerci, B. Wood, *Proc. ASME Adv. Energy Syst. Div.* **1999**, *39*, 537 – 543; b) Y. Cerci, Y. A. Cengel, B. Wood, *Proc. ASME Adv. Energy Syst. Div.* **1999**, *39*, 545 – 552.
[7] B. Peñate, L. García-Rodríguez, *Desalination* **2012**, *284*, 1 – 8.
[8] A. J. Bard, *Integrated chemical systems: a chemical approach to nanotechnology*, Wiley, New York, NY, **1994**.
[9] R. Dhopeshwarkar, D. Hlushkou, M. Nguyen, U. Tallarek, R. M. Crooks, *J. Am. Chem. Soc.* **2008**, *130*, 10480 – 10481.
[10] D. R. Laws, D. Hlushkou, R. K. Perdue, U. Tallarek, R. M. Crooks, *Anal. Chem.* **2009**, *81*, 8923 – 8929.
[11] E. Sheridan, K. N. Knust, R. M. Crooks, *Analyst* **2011**, *136*, 4134 – 4137.
[12] K. Scida, E. Sheridan, R. M. Crooks, *Lab Chip* **2013**, *13*, 2292 – 2299.
[13] F. Mavré, R. K. Anand, D. R. Laws, K.-F. Chow, B.-Y. Chang, J. A. Crooks, R. M. Crooks, *Anal. Chem.* **2010**, *82*, 8766 – 8774.
[14] a) D. Hlushkou, R. K. Perdue, R. Dhopeshwarkar, R. M. Crooks, U. Tallarek, *Lab Chip* **2009**, *9*, 1903 – 1913; b) R. K. Perdue, D. R. Laws, D. Hlushkou, U. Tallarek, R. M. Crooks, *Anal. Chem.* **2009**, *81*, 10149 – 10155; c) R. K. Anand, E. Sheridan, D. Hlushkou, U. Tallarek, R. M. Crooks, *Lab Chip* **2011**, *11*, 518 – 527.
[15] K. N. Knust, E. Sheridan, R. K. Anand, R. M. Crooks, *Lab Chip* **2012**, *12*, 4107 – 4114.
[16] Z. Huang, C. F. Ivory, *Anal. Chem.* **1999**, *71*, 1628 – 1632.
[17] P. H. Humble, R. T. Kelly, A. T. Woolley, H. D. Tolley, M. L. Lee, *Anal. Chem.* **2004**, *76*, 5641 – 5648.
[18] S. J. Kim, Y.-A. Song, J. Han, *Chem. Soc. Rev.* **2010**, *39*, 912 – 922.
[19] S. J. Kim, S. H. Ko, K. H. Kang, J. Han, *Nat. Nanotechnol.* **2010**, *5*, 297 – 301.
[20] M. E. Suss, T. F. Baumann, W. L. Bourcier, C. M. Spadaccini, K. A. Rose, J. G. Santiago, M. Stadermann, *Energy Environ. Sci.* **2012**, *5*, 9511 – 9519.
[21] M. Pasta, C. D. Wessells, Y. Cui, F. La Mantia, *Nano Lett.* **2012**, *12*, 839 – 843.
[22] M. Sadrzadeh, T. Mohammadi, *Desalination* **2008**, *221*, 440 – 447.
[23] Y. Oren, *Desalination* **2008**, *228*, 10 – 29.
[24] S. Ranganathan, R. McCreery, S. M. Majji, M. Madou, *J. Electrochem. Soc.* **2000**, *147*, 277 – 282.
[25] G. M. Geise, H.-S. Lee, D. J. Miller, B. D. Freeman, J. E. McGrath, D. R. Paul, *J. Polym. Sci. Part B* **2010**, *48*, 1685 – 1718.
[26] J. E. Bennett, *Int. J. Hydrogen Energy* **1980**, *5*, 401 – 408.
[27] E. R. Carraway, J. N. Demas, B. A. DeGraff, J. R. Bacon, *Anal. Chem.* **1991**, *63*, 337 – 342.
[28] M. Elimelech, W. A. Phillip, *Science* **2011**, *333*, 712 – 717.

